Modelling and Analysis of Transformer Winding at High Frequencies

Yoshikazu Shibuya, *nonmember*, Takuto Matsumoto, *nonmember*, Tsuneharu Teranishi, *member, IEEE*

Abstract--Circuit models of interlinked inductances and capacitances have been widely used to analyse the transformer transients caused by lightning or switching surges. A winding model applicable to higher frequencies is required in order to analyse the effects of very fast transients (VFT) due to the disconnecting switch surges originated in gas insulated switchgear (GIS).

An improved procedure is proposed here, in which the circuit constants are evaluated on turn-to-turn basis directly from the geographical dimensions of transformer winding. This method is applicable to the interleaved coils as well as the continuous ones. To avoid the number of turns or nodes becoming too large, a technique of grouping turns is implemented. The transient analysis is performed using the Electromagnetic Transients Program (EMTP). The input data file is created automatically from the winding geometry assuming adequate dissipation parameters with the use of a specially developed program.

The applicability of this method is verified by the experiments involving two kinds of model windings, one interleaved and another continuous, in which internal voltages are observed applying pulses of rising time as short as 30 ns. The correspondence with the analytical results is satisfactory. The experimental and analytical show a reasonable agreement also in the frequency domain.

The present method is expected to be useful in assessing the VFT vulnerability of a transformer. This can be done in the designing stage prior to actual manufacturing since only the winding geometry is necessary for the analysis.

Keywords: Very fast transient overvoltage, Transformer model, High frequency, Transient analysis, EMTP

I. Introduction

LUMPED circuit models have been commonly used to analyse the transformer transients associated with the lightning or switching surges [1]-[6]. In the lumped model, the winding is divided into a number of parts usually into coil section-pairs. However, this is insufficient to calculate the influences from the disconnecting switching surges or the very fast transient overvoltage (VFTO) generated in GIS [7]-[14]. For this kind of frequency analysis, the multiconductor transmission-line (MTL) model is proposed [7], and successfully applied to the shell-type transformer [8]-[10]. This method is rather difficult to be applied to the core-type in which complex interleaved winding is often used.

In order to simulate the high frequency transients of core-type transformer, one of the present authors has used a section-pair circuit model comprising a resistance representing the surge impedance of winding assuming its distributed-line-like behaviour [11], [12]. Another of the authors has shown that a turn-to-turn lumped circuit modelling is advantageous for high frequency simulation [13]. The parameters calculated from the winding geometry are used in the frequency domain circuit calculation based on the matrix technique. However, this method involves the cumbersome inverse Fast Fourier Transformation (FFT) to obtain time-domain results.

If this turn-to-turn base lumped circuit model is implemented in the EMTP, the time-domain calculation will be conducted with much ease. A special program is developed, which automatically produces the EMTP input data directly from the winding's geometry and material constants.

In this paper, the EMTP-analysed results are compared with the experimental data in which the real-size transformer windings are applied with very fast pulses.

II. Equivalent Circuit

A. Shape of Winding

Fig. 1 shows the core-type transformer in which the high voltage (HV) winding is placed outside the low voltage (LV) winding. The HV winding is composed of a number of disk-shaped coil sections and the static plates (SP) fixed at coil ends, which are not always employed. A high frequency surge shall appear at the top of HV winding when VFTO occurs.

There are two types of winding as shown in Fig. 2 — one

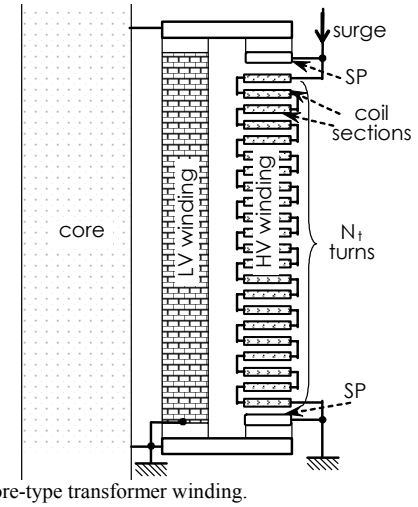

Fig. 1. Core-type transformer winding.

Y. Shibuya is with the Department of Electrical Engineering, Shibaura Institute of Technology, 3-9-14 Shibaura, Minato-ku, Tokyo 108-8548, Japan (e-mail: shibuya@iee.org).

T. Mastumoto is with the East Japan Railway Company, Tokyo, Japan.

T. Teranishi is with Power Transformer Division, Toshiba Corporation, 2-1 Ukishima-cho, Kawasaki-ku, Kawasaki 210-0862, Japan.

Presented at the International Conference on Power Systems Transients (IPST'05) in Montreal, Canada on June 19-23, 2005
Paper No. IPST05-025

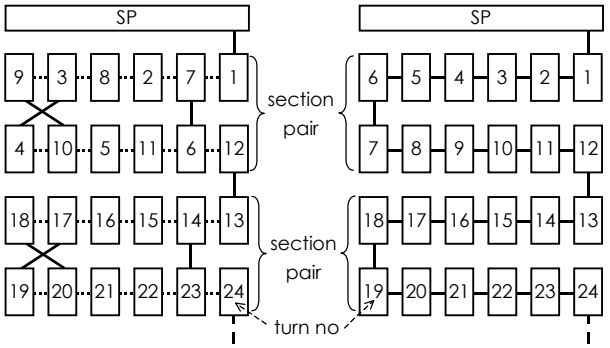

(a) Interleaved (b) Continuous

Fig. 2. Two winding types used in core-type transformer.

is the interleaved winding to improve the capacitive voltage distribution, and another is the continuous one. In both cases, a pair of coils or section-pair is considered as the unit of HV winding. This section pair has been treated as inseparable unit in the models used hitherto. If the individual turn is taken as the unit, a model more suitable for higher frequency analysis will be realised.

The followings are the steps to construct turn-to-turn base inductances and capacitances and then to use them to obtain the constants for a more degenerated lumped circuit model. The two types: interleaved and continuous can be treated in a similar manner.

B. Inductance

The self-inductance of individual turn is calculated by the following equation, if it is looked as a straight conductor of equal section and length as shown in Fig. 3a.

$$L_{ii} = \frac{\mu_0 \ell}{2\pi}\left(\ln\frac{2\ell}{R} - 1\right) \tag{1}$$

Where, R is the geographical mean diameter (GMD), which can be estimated if the current distribution is assumed — authors used four even currents at the conductor corners [13].

Mutual inductances are evaluated as that between two rings neglecting the existence of other conductors:

$$L_{ij} = \mu_0 \sqrt{r_i r_j}\left\{\left(\frac{2}{k} - k\right)K(k) - \frac{2}{k}E(k)\right\} \tag{2}$$

Where, $K(k)$ and $E(k)$: the perfect elliptic integrals of first and second kinds, $k^2 = 4\ r_i\ r_j/\{(r_i + r_j)^2 + z^2\}$: as for r_i, r_j, z, see Fig. 3b. This means that the presence of core is neglected assuming it does not enhance or suppress the magnetic flux at the high frequency [13].

The turn-to-turn base inductances L_{ij} for all the turns are calculable by (1) and (2). The matrix, if formed, would be a dense matrix with dimension N_t, the total number of turns, usually a very large number.

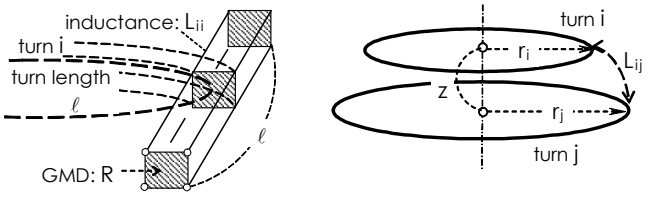

(a) Self-inductance (b) Mutual inductance

Fig. 3. Assumptions in calculating inductances.

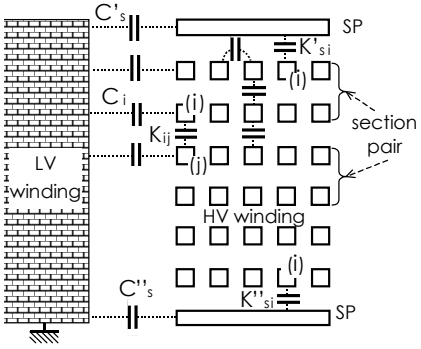

Fig. 4. Capacitances evaluated by parallel-plate approximation.

Capacitances

The following capacitances shown in Fig. 4 are considered to be significant.

(a) turn-ground, SP-ground: C_i, C'_s, C''_s

(b) turn- turn, SP-turn: K_{ij}, K'_{si}, K''_{si}

They are in the positions with conductors facing each other. LV winding is regarded as a ground surface for simplicity. All the capacitances can be evaluated by the parallel-plane approximation. For instance,

$$K_{ij} = \varepsilon_s \varepsilon_0 \frac{W \cdot \ell}{d} \tag{3}$$

Where, d, W and ℓ are the insulation thickness, width and turn length. The dielectric constant ε_s can be differentiated according to the insulation materials of relevant local space. For example, different values of ε_s can be set for turn-turn, section-section, and HV-LV capacitances [13].

C. Model with Reduced Number of Nodes

It is possible to model the transformer winding on turn-to-turn base using the inductances and capacitances mentioned above. The total number of turns N_t may be large as 1000 in ordinary transformers. The number of nodes, therefore, is likely to exceed 400, the upper limit in the number of "mutually coupled R-L elements" of EMTP.

The technique of reducing the number of nodes has been introduced previously in the analysis using FFT [13]. There, turns are grouped into a smaller number of subgroups within the section pair. Consequently, the number of nodes can be reduced from the initial level of N_t. Fig. 5 shows the equivalent circuit thus derived. Let N be the total number of divisions, inductances are expressed by a matrix $[L]$ of dimension N. It should be noted that the values of inductances $[L]$ and capacitances K's, C's can be calculated simply summing up the turn-to-turn base inductances and capacitances.

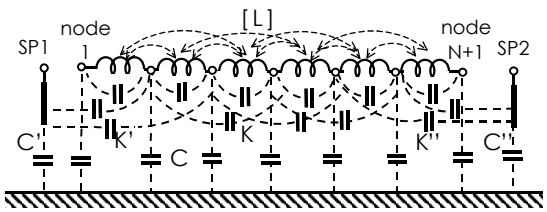

Fig. 5. Equivalent circuit of transformer winding at high frequencies.

D. Resistances Representing Dissipations

Dissipations at high frequencies are thought to be caused not only by the resistance in the winding conductor but also by the dielectric loss in the insulation. Introducing adequate resistances to the equivalent circuit is essential in realising a transformer model to be used in VFT analysis.

Fig. 6 shows how the power factor of inductance model with series resistance varies with frequency for two cases. One case (a) is for a fixed value resistance, and (b) is for the frequency-dependent resistance with the skin effect taken into account. In the latter, the current is assumed to flow only within the skin depth δ from the conductor surface. The resistance becomes a function of frequency f: $r_{skin}(f)$, since δ depends on ω (=$2\pi f$) and the conductor conductivity σ in the way:

$$\delta = \sqrt{\frac{2}{\mu_0\ \omega\ \sigma}} \qquad (4)$$

Where, the permeability is set to be equal to that of vacuum μ_0. Although the frequency dependent resistance can be easily accommodated in FFT analysis [13], it is difficult to be implemented in EMTP analysis. In the present analysis, r is set to be constant with frequency, the value being equal to that of (b) at a frequency f_0 (i.e. r=$r_{skin}(f_0)$).

Fig. 7 shows how the power factor of dissipative capacitance varies with frequency for the three models. Models (a) and (b) are the cases that a fixed value resistance is assumed in parallel and in series, respectively. The constant power factor (c) is equivalent to the case that the loss tangent tanδ of insulation is kept constant in the frequency range. The admittance of this capacitance K is expressed in the form:

$$Y = j\,\omega K + \omega K \tan\delta \qquad (4)$$

This case (c) corresponds to the condition of the FFT analysis in [13]. However, in EMTP analysis, either (a) or (b) has to be chosen. A similar fitting parameter f_0 is used so that the power factor becomes equal to the specified loss tangent tanδ at the frequency f_0.

Most of the current passes through C rather than through L at high frequencies. Therefore, the resistance r series to L little contributes to the dissipations at high frequency in the present model. Since the dielectric loss is dominant, the selection of its dissipation model is more important, namely the selection between the parallel- or series- resistance models as well as the values of tanδ and f_0. However, these are difficult to be determined because of lack in basic data concerning the high frequency dielectric loss. Therefore, the feasibility of those two models is evaluated by the results of simulation assuming appropriate dissipation parameters.

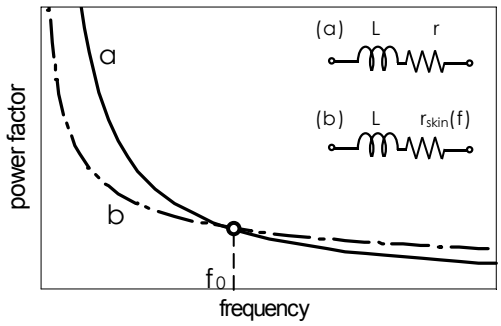

Fig. 6. Power factor of inductance-resistance circuit: (a) with fixed resistance and (b) with frequency-dependent resistance regarding skin effect.

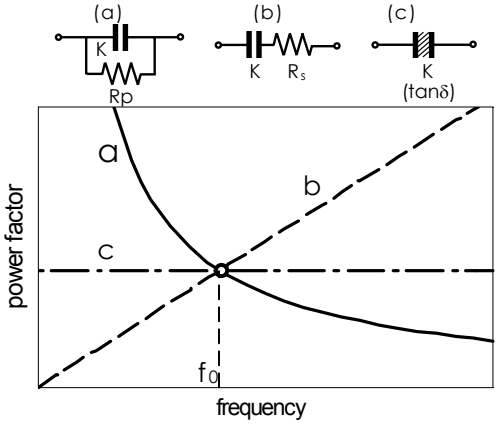

Fig. 7. Power factor of dissipative capacitance circuit: (a) parallel resistance model, (b) series resistance model, and (c) constant tanδ model.

III. EMTP Analysis

A. Automatic Creation of EMTP Data File

The high frequency model of Fig. 5 including the dissipation resistances can be brought into EMTP if the following 'branch cards' [15] are prepared.

1) : Mutually-coupled R-L elements

The elements of matrix [L] and resistances r are written in the specific format.

2) : Uncoupled, lumped, series R-L-C branches

The capacitances K's, C's, and resistances R_p (or R_s) are written in the specific format.

In both cases, the parameters cannot be set manually because the number of parameters is large. A special Windows program is developed, in order to create those branch cards automatically. Fig. 8 shows the flow chart. The constants are calculated directly from the transformer's geometrical and other necessary data. It is possible to check the transformer's configuration and available nodes by the use of graphics.

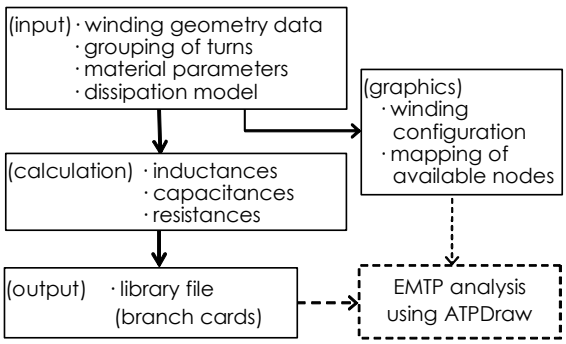

Fig. 8. Flow chart for creating library file to be used in ATPDraw.

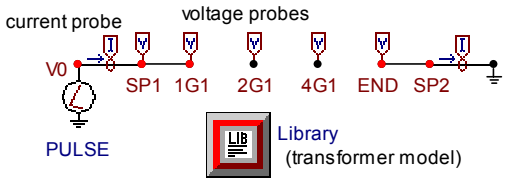

Fig. 9. Use of 'library object' in ATPDraw to execute EMTP.

B. Analysis using ATPDraw

If the 'library object' in ATPDraw [16] is assigned to the file of branch cards (named as 'library file' in Fig. 8), the transient voltages or currents can be obtained simply by quoting the relevant node names at the 'probes'.

Fig. 9 is an example that voltages and currents are observed at several points when a pulse is applied. The node names have to be identical to those provided by the program of Fig. 8. The names can be checked by the graphics. For example, nodes SP1, SP2 represent SPs, and nodes 1G1, · · · , END, the turn positions from the beginning to the end of winding.

IV. Analysed Windings and Their Parameters

A. Transformer Windings Analysed

The present analysing method is applied to the two model transformer windings of practical-size. Table I shows the outline of those models: Windings C and H are the continuous and interleaved types, respectively. Both windings have the same number of sections but the number of turns of Winding H is twice larger than Winding C.

TABLE I
Transformer Windings Used in Experiment and Analysis

Winding		C	H
type		continuous	interleaved
static plates		no	no
number of sections		40	40
total number of turns		320	640
size (m)	diameter	0.87	0.92
	height	0.88	0.76

B. Dissipation Parameters

Fig. 10 shows the frequency characteristics of input impedance for winding C for the four cases:

(a) Frequency-constant resistance r in series for L and constant parallel resistance R_p for C.
(b) Constant series resistance r for L, and constant serial resistance R_s for C.
(c) Frequency-variable series resistance $r_{skin}(f)$ for L (σ=5×10^7 S/m), and constant tanδ (=0.05) for C.
(d) Experimentally obtained.

The resistances are so chosen to give the same power factor at f_0 (set 0.3 and 0.1 MHz, for 'a' and 'b', respectively). Both 'a' and 'b' are calculated using 'frequency scan' of EMTP, 'c' is obtained from the FFT calculation method described in [13], and 'd' is obtained using a network analyser.

Comparing the curves 'a' and 'b' in Fig 10, 'a' better resembles the measured 'd', since the resonant kinks are less pronounced at high frequencies. In the following calculations, the constants are calculated for constant series resistance model (b) with:

σ=5×10^7 S/m, tanδ=0.05, f_0=0.1 MHz.

C. Effect of Grouping Turns

The curves 'a' and 'b' in Fig 10 are calculated without grouping turns (i.e. turn-to-turn modelling). Fig. 11 shows how reducing the number of divisions influences the frequency characteristics. The three curves do not differ in the frequency range lower than 0.5 MHz, but differences appear at higher frequencies. It is speculated that grouping several turns to the extent of about 5 m length may not significantly affect the calculated results in the frequency range up to 1 MHz.

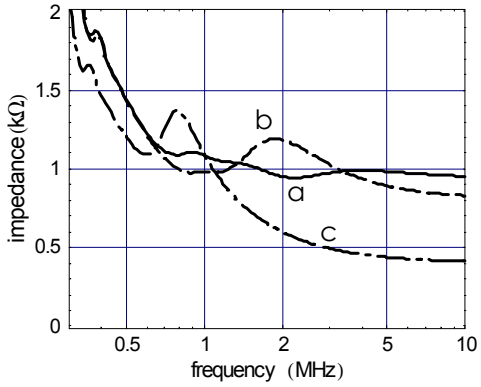

Fig. 11. Effect of grouping turns on high-frequency characteristics of input impedance for winding C. Number of divisions: (a) 320, (b) 120, (c) 40.

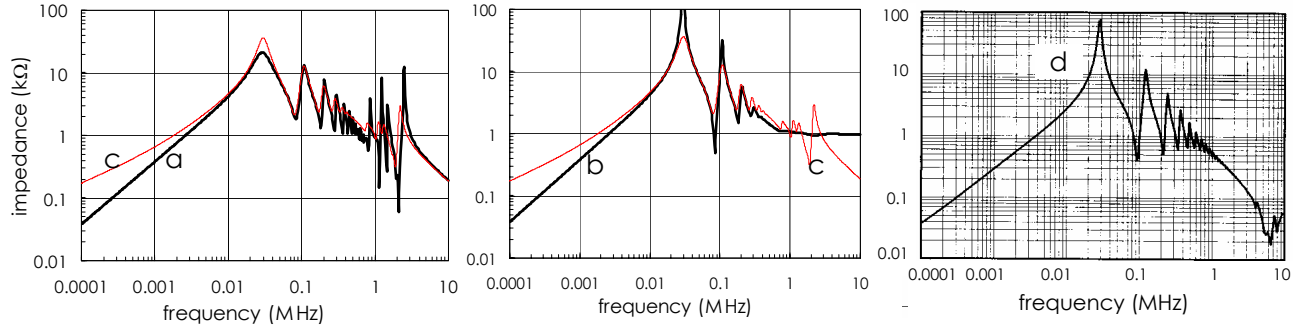

Fig. 10. Frequency characteristics of input impedance for winding C. Capacitance's dissipation models: (a) constant parallel resistance (f_0=0.3 MHz), (b) constant serial resistance (f_0=0.1 MHz), and (c) constant tanδ (=0.05); and (d) experimental.

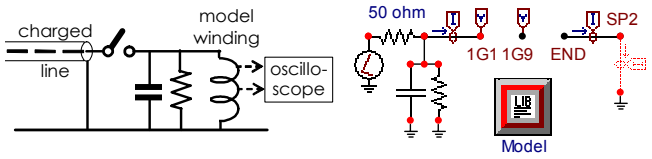

(a) Experimental (b) ATPDraw circuit

Fig. 12. Application of impulse to model winding.

V. Time Domain Results

In the experiment, a low impulse voltage is applied to the model winding by the line discharge. The voltages induced in the winding are observed using the circuit shown in Fig. 12a [12]. This transient is analysed using the ATPDraw circuit shown in Fig. 12b.

A. Voltage Oscillations

Voltage oscillations occur when an impulse voltage is applied to the transformer winding. Transients are observed experimentally when the two model windings are subjected to the standard impulse voltage with the rising time of 1.2 μs. They are compared with the analysed results.

Figs. 13 and 14 compare the analysed results with corresponding experimental, for Windings C and H, respectively. The voltages of some uppermost sections are shown. It is noted that the response of interleaved winding is faster than that of continuous type as expected.

Comparing the simulation and experimental, the shapes of wave front are almost the same, although there exist some extra oscillations in the simulation.

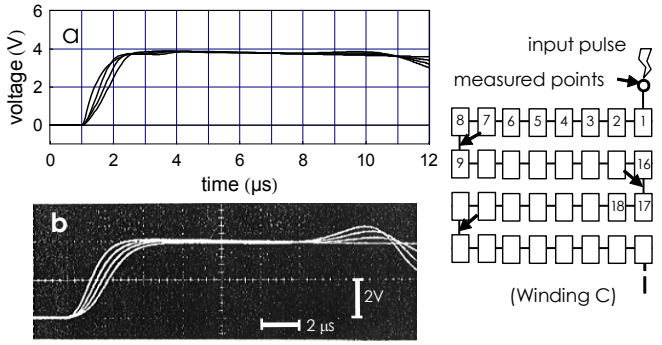

Fig. 13. Voltage oscillations of continuous Winding C subjected to standard impulse with rising time of 1.2 μs: (a) simulation, and (b) experimental.

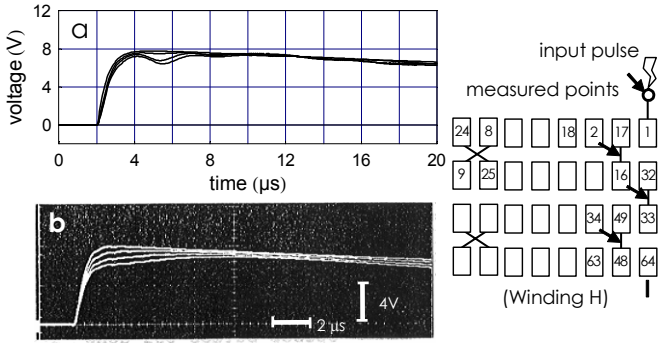

Fig. 14. Voltage oscillations of interleaved Winding H subjected to standard impulse with rising time of 1.2 μs: (a) simulation, and (b) experimental.

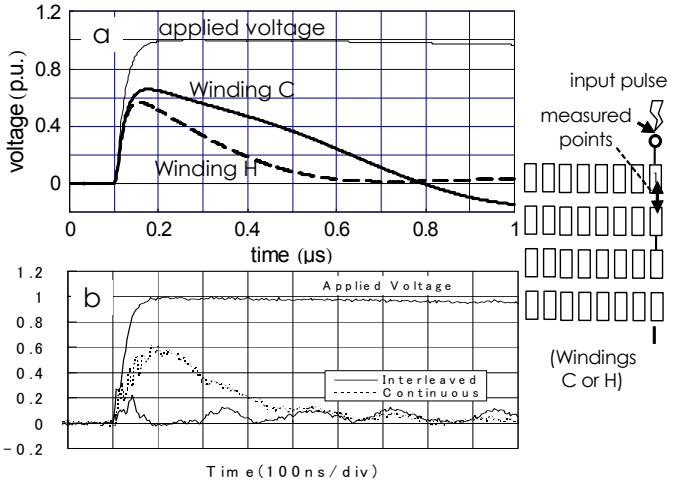

Fig. 15. Inter-section voltages of Windings C and H subjected to impulse with rising time of 70 ns: (a) simulation, and (b) experimental.

B. Inter-Section Voltages

The inter-section voltage has been observed experimentally [12] in order to investigate the effect of VFT on the local voltage near the HV entrance. Fig. 15 shows the results using 70 ns rising-time impulse, in which the experimental results are compared with those of simulation.

It is assured that the initially induced voltage level is smaller for interleaved in both results. The simulation gives larger voltage levels.

C. Interturn Voltages

Fig. 16b shows how a very fast impulse of 70 ns rising-time induces abnormal voltages in the first two interturns in the case of Winding H. This reflects the nature of VFTO inducing a large interturn voltage in the vicinity of entrance.

In the simulation shown in Fig. 16a, similar initial abrupt changes are seen in the voltages 2 and 3. Here again, the simulation gives somewhat larger voltage levels.

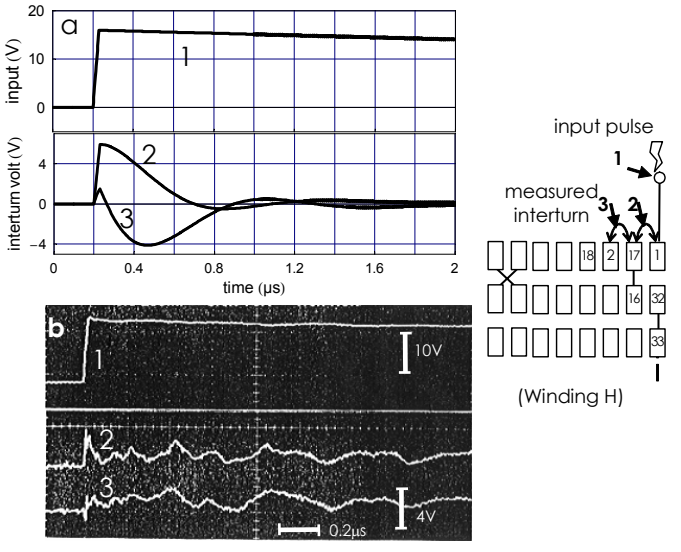

Fig. 16. Interturn voltages of Winding H subjected impulse with rising time of 30 ns: (a) simulation, and (b) experimental.

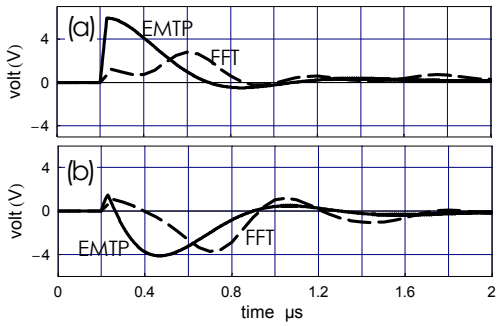

Fig. 17. Interturn voltages obtained by EMTP (same as Fig. 16a) compared with those by FFT. (a) and (b): first and second interturn voltages

D. Comparison with FFT analysis

The simulation utilising FFT [13] is applicable to the same problem. Fig. 17 compares EMTP results with FFT for the interturn voltages shown in Fig. 16. It is justifiable that EMTP gives a sharper initial voltage rise than the FFT which assumes a continuous curve. It may be that EMTP analysis gives more realistic results for VFT situations.

VI. CONCLUSIONS

According to the present method, one can determine the inductances and capacitances of the transformer winding model on turn-to-turn basis. The library file for EMTP simulation can be created from the geometry data of HV winding, material constants and dissipation model by the use of specially developed program. It can be readily used as a usual circuit element in EMTP analysis.

Utilising EMTP, particularly ATPDraw, assures a versatile circuit-building. This is the practical merit compared to using the FFT analysis previously reported

Since the present analysis can be done based on the winding geometry, this method is expected to be useful in assessing the VFT vulnerability of a transformer in the designing stage prior to actual manufacturing. On the other hand, a better dissipation model is clearly needed for more accurate, qualitative simulation. This will be pursued in the future.

VII. REFERENCES

[1] P. A. Abetti, "Bibliography on the surge performance of transformers and rotating machines", *Trans. AIEE*, vol.77, 1958, pp.1150-1168.

[2] A. Greenwood, *Electrical Transients in Power Systems*, pp.322-346, John Wiley & Sons, New York 1991.

[3] J. H. McWhirter, C. D. Fahrnkoph, and J. H. Steele, "Determination of impulse stresses within transformer windings by computers", *Tran. of AIEE*, vol.76 Pt.III, 1957, pp.1267-1274.

[4] W. J. McNutt, T. J. Blalock, and R. A. Hinton, "Response of transformer windings to system transient voltages", *IEEE Trans. Power Apparatus and Systems*, vol.PAS-93 (2), 1974, pp. 475-467.

[5] R. C. Degeneff, "A general method for determining resonances in transformer windings", *IEEE Trans. Power Apparatus and Systems*, vol.PAS-96, 1977, pp. 423-430.

[6] D. J. Wilcox, W. G. Hurley, T. P. McHale, and M. Conlon, "Application of modified modal theory in the modelling of practical transformers", *Proc. of IEE*, vol.139 Pt.C (6), 1992, pp. 513-520.

[7] K. Cornick, B. Filliat, C. Kieny, and W. Müller, "Distribution of very fast transient overvoltages in transformer windings", *CIGRE Report*, 12-204, 1992.

[8] Y. Shibuya, S. Fujita, and N. Hosokawa, "Analysis of very fast transient overvoltage in transformer winding", *IEE Proc. Generation Transmission and Distribution*, vol.144, No.5, 1997, pp.461-468.

[9] Y. Shibuya, S. Fujita, and E. Tamaki, "Analysis of very fast transients in transformer", *IEE Proc. Generation Transmission and Distribution,* vol.148, No.5, 2001, pp.377-383.

[10] Y. Shibuya, S. Fujita, and E. Tamaki, "Analysis of very fast transients in transformer", *IPST'2001*, Rio de Janeiro, Brazil, 24-28 June, 2001, pp.98-103.

[11] S. Okabe, M. Koto, T. Teranishi, M. Ishikawa, T. Kobayashi, and T. Saida, "An electric model of gas-insulated shunt reactor and analysis of re-ignition surge voltages", *IEEE Trans. Power Delivery*, vol.14, No.2, 1999, pp.378–386

[12] S. Takahashi, T. Inoue, T. Teranishi, and M. Ikeda, "Overvoltages in transformer windings under very fast transients", *ICEE'99*, 1999, Hong Kong.

[13] Y. Shibuya, and S. Fujita, "High frequency model of transformer winding", *Electrical Engineering in Japan* vol.146, No.3, 2004, pp.8-15.

[14] S. Fujita, N. Hosokawa and Y. Shibuya, "Experimental study of very fast transient phenomena in transformer winding", *IEEE Trans. Power Delivery*, Vol.13, No.4, 1998, pp.1201-1207.

[15] Leuven EMTP Center (LEC), *Alternative Transients Program Rule Book*, p.4A1, p.4C-1, 1987.

[16] L. Prikler, H. K. Høidalen, *ATPDRAW version 3.5 Users' Manual*, *Preliminary Release No. 1.1*, p.124, 2002

VIII. BIOGRAPHIES

Yoshikazu Shibuya was born in 1941. He graduated from Kyoto University in 1964. He received MS from Kyoto University and PhD from University of Salford, UK, in 1966 and 1974, respectively.

He was with Central Research Laboratory, Mitsubishi Electric Corporation from 1966 to 1999. His field is the fundamental insulation technique relating various high voltage power apparatuses such as GIS and transformer. He is a professor at Shibaura Institute of Technology since 1999. Dr Shibuya is a member of IEE and IEE of Japan.

Takuto Matsumoto was born in 1981. He received B.S., M.S. from Shibaura Institute of Technology in 2003, 2005, respectively. He is with East Japan Railway Company from April, 2005.

He has been engaged in the research on the analysis of high frequency phenomena in transformer winding while he was a graduate student in Shibaura Institute of Technology.

He is a Member of IEE of Japan.

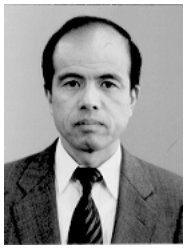

Tsuneharu Teranishi was born in 1946. He received his B.S., M.S., and Ph.D degrees in electrical engineering from Nagoya University in 1968, 1970, and 1983 respectively. In 1973, he joined the Transformer Department at Hamakawasaki Works of Toshiba Corporation, and has been engaged in the development of power transformers. He is a member of IEEE and IEE of Japan.